Stochastic analysis of vortex-induced vibrations by means of a randomized wake-oscillator model

Vincent Denoël

University of Liège, Liège, Belgium, v.denoel@uliege.be

Abstract

The influence of wind turbulence on the vortex-induced response of a single cylinder is not well understood yet. It also appears that there is no commonly accepted model to represent the influence of a turbulent flow. In this paper, a low-order phenomenological model, inspired by the smooth flow VIV model derived by Facchinetti *et al.*, is described and analyzed. The main features of this model are presented. In particular, the topology of the limit cycle of the coupled wake-oscillator system is analyzed in the presence of noise. The extent of the so-called lock-in domain is interpreted, in the stochastic version of the problem, by means of the statistics of the phase between the two degrees-of-freedom. Based on the slow phase model of the problem, it is shown that both the turbulence intensity and the frequency content of the turbulence play a significant role in the statistical distributions of the magnitudes of fluid and structure oscillations. The derivation is proposed in a dimensionless version so that the major scalings driving the problem naturally come out of the analysis.

Keywords: Vortex induced vibrations (VIV), Facchinetti-De Langre-Biolley model, random synchronization, stochastic Van der Pol oscillator, lock-in range, turbulence

1 Introduction

There exist three families of models to describe vortex-induced vibrations (VIV) of bodies immersed in smooth flows (Païdoussis et al. 2010). They are typically classified as externally forced models, modified or state-dependent forced models and coupled fluid-structure models (Facchinetti et al. 2004, Tamura 1981). The available mathematical models to describe VIV in a turbulent flow are much scarcer, albeit most of the civil engineering applications take place in the atmospheric boundary layer where the magnitude of the fluctuating component can reach up to 20% or more of the average wind velocity. Experimental evidences (Goswami et al. 1993) and computational fluid dynamics simulations (NGuyen et al. 2018) have studied the influence of turbulence on vortex-induced vibrations and revealed it is a somewhat complicated problem. There are some needs, though, for simple models of VIV in the presence of noise. In the family of externally forced models, Vickery and coworkers (Vickery and Clar, 1972; Vickery and Basu, 1983) have proposed a loading model of tapered stacks which is still widely used today. It constitutes a cornerstone of the modeling of turbulence on vortex-induced vibrations. This model has been constructed as a simple generalization of the externally forced model (family 1), by modeling the aerodynamic loading as a narrow band stochastic process, instead of a deterministic harmonic loading. Following the same spirit, this paper presents and analyzes a randomized version of a simple wake oscillator model (family 3). Such a model has already been used in Monte Carlo simulation conditions, see eg. (Mannini, 2016). The main contribution of this exposé is therefore related to the analysis of the model with the pragmatical tools of nonlinear stochastic dynamics. This paper is a condensed version of a full scientific archive which is sill under review (Denoël, 2020).

2 Considered wake-oscillator model

The Facchinetti–de Langre–Biolley (FDLB) model reads (Facchinetti et al. 2004)

$$(m_S + m_F)\,\ddot{y} + \left(c_S + \tfrac{C_D}{2}\rho U_\infty D\right)\dot{y} + k_S y = \frac{1}{4}\rho U_\infty^2 D C_L^0 q \tag{1}$$

$$\ddot{q} + 2\pi St \tfrac{U_\infty}{D}\varepsilon\,(q^2-1)\,\dot{q} + \left(2\pi \mathrm{St}\tfrac{U_\infty}{D}\right)^2 q = 2\mathcal{A}_0\frac{\ddot{y}}{D} \tag{2}$$

where $y(t)$ (units: L) and $q(t)$ (units: -) represent the two degrees-of-freedom associated with the cross-flow structural motion and the lift force resulting from vortex shedding. The parameters of the model are m_S, c_S and k_S, the mass, viscosity and stiffness of the structure (per unit length), D the cylinder diameter (or characteristic cross-flow dimension), ρ and U_∞ the density and the constant fluid velocity, C_D and C_L^0 the stationary drag and lift coefficients on the fixed body and St the Strouhal number. Finally $\mathcal{A}_0$ is a dimensionless parameter related to the influence of the structural motion on the dynamics of the wake ($2\mathcal{A}_0$ is represented by symbol A in Facchinetti et al. 2004), while ε is another dimensionless parameter that describes the memory in the wake equation and is related to the magnitude of the nonlinearity in the Van der Pol equation for the wake, therefore to the strength of the limit cycle. The equivalent mass of displaced fluid $m_F = C_M \rho D^2 \frac{\pi}{4}$ (which is negligible in wind engineering applications) is added to the structural mass m_S in order to define the structural circular frequency $\omega_0 = \sqrt{k_S/(m_S+m_F)} = \sqrt{k_S/m}$.

A dimensionless version of the governing equations is obtained by introducing

$$\xi_s = \frac{c_S}{2\sqrt{k_S m}}, \quad \xi_a = \frac{\rho U_\infty D}{4\sqrt{k_S m}} C_D, \quad \Omega = \frac{\mathrm{St}\,U_\infty/D}{\omega_0/2\pi} = \frac{f_{\mathrm{shedding}}}{f_0}, \quad \mu = \frac{\rho\pi D^2}{4m} = \frac{\rho}{\rho_S}, \tag{3}$$

characterizing the structural damping ξ_s and aerodynamic damping ξ_a , as well as a the reduced wind velocity Ω and the mass ratio μ (where ρ_S the equivalent density of the cylinder). With these notations, the governing equations read

$$\mathcal{Y}'' + 2\,(\xi_s+\xi_a)\,\mathcal{Y}' + \mathcal{Y} = 2\varepsilon\mathcal{M}_0\Omega^2\mathcal{Q} \tag{4}$$

$$\mathcal{Q}'' + \varepsilon\,\Omega\left(\mathcal{Q}^2-1\right)\mathcal{Q}' + \Omega^2\mathcal{Q} = 2\varepsilon\mathcal{A}_0\mathcal{Y}'' \tag{5}$$

where $\mathcal{Y}(\tau) = \frac{y[t(\tau)]}{\varepsilon D}$ and $\mathcal{Q}(\tau) = q\,[t(\tau)]$ and where the prime symbol denotes derivatives with respect to the dimensionless time $\tau = \omega_0 t$. The parameter $\mathcal{M}_0$, defined as

$$\mathcal{M}_0 := \frac{\mu}{8\pi^3\varepsilon^2}\frac{C_L^0}{\mathrm{St}^2}$$

carries information about the mass ratio, the magnitude of the lift force, the reduced frequency and the shape of the body (through the Strouhal number and lift coefficient). It is related to the Skop-Griffin parameter because it is the sole dimensionless group of this model related to the mass ratio μ. In this paper, we assume that the mass ratio is a small number, which typically suits well wind engineering applications. As a consequence, $\mathcal{M}_0$ is order 1 at most. This is the same for $\mathcal{A}_0$. The governing equation therefore features small coupling terms, which is typical in synchronization problems (Pikovsky at al. 2003).

The turbulence of the oncoming flow is introduced in the model, following the quasi-steady approach. A randomized version of the governing equations is obtained by substituting $U_\infty + u(t)$ for U_∞ in the previous equations. It is assumed that $u(t)$ is a zero-mean Gaussian stochastic process with known variance σ_u and known power spectral density S_u (PSD). As usual in wind engineering applications, it is also assumed that the turbulence intensity $I_u = \sigma_u/U_\infty$ is a small number. A dimensionless turbulence $\mathcal{U}(\tau) = u\left[t\left(\tau\right)\right]/\sigma_u$ is also defined in order to fit the framework of the dimensionless formulation. Following the definition of $\mathcal{U}(\tau)$, its power spectral density is given by $S_{\mathcal{U}}\left(\tilde{\omega};\alpha\right) = \frac{\omega_0}{\sigma_u^2} S_u\left(\tilde{\omega}\,\omega_0;\alpha\,\omega_0,\sigma_u^2\right)$ where $\tilde{\omega} = \omega/\omega_0$ is the dimensionless frequency parameter (associated with time τ) and $S_u\left(\omega;\alpha\omega_0,\sigma_u^2\right)$ is the power spectral density of $u(t)$, and where α a dimensionless characteristic frequency of the turbulence velocity typically used in the multiple scale analysis of buffeting. This later parameter is typically much smaller than 1 in wind engineering applications; it is the ratio of the characteristic frequency of wind [~0.005 Hz or less] to the structural natural frequency [0.5-3 Hz or more], see details in (Denoël and Carassale, 2015)

3 Models for the stochastic wake-oscillator

3.1 The Original model

After considering the smallness of the turbulence intensity I_u, substitution of $\mathcal{U}(\tau) = u\left[t\left(\tau\right)\right]/\sigma_u$ into the governing equations yields a first stochastic version of the problem, hence called the *original* model,

$$\begin{aligned} \mathcal{Y}'' + 2\xi\mathcal{Y}' + \mathcal{Y} &= 2\varepsilon\mathcal{M}_0\Omega^2\mathcal{Q} \\ \mathcal{Q}'' + \varepsilon\,\Omega\left(\mathcal{Q}^2 - 1\right)\mathcal{Q}' + \Omega^2\left(1 + 2I_u\mathcal{U}\right)\mathcal{Q} &= 2\varepsilon\mathcal{A}_0\mathcal{Y}''. \end{aligned} \tag{6}$$

This model is obtained by assuming $\{I_u, \xi, \varepsilon\} \ll 1$, which allowed to consider as secondary the several occurrences of $\mathcal{U}(\tau)$ in the governing equations after a formal substitution. Equations (6) indicate that, at leading order, the turbulence mainly affects the reversible forces of the fluid oscillator. This set of equations serves as a reference model. The numerical solution of this model under typical turbulent flow will be used later to assess the quality of simple analytical solutions derived with the two following models.

3.2 The Averaged model

A first simplified model, called the *averaged* model, is obtained by means of a perturbation analysis of (6). Standard techniques in multiple timescale analysis (Hinch 1991), first require to recognize the existence of small numbers, namely $\{I_u, \xi, \varepsilon\}$, which is formalized by introducing

$$I_u = \mathcal{I}_0\varepsilon \quad ; \quad \xi = \xi_s + \xi_a = \xi_0\varepsilon \tag{7}$$

in order to be able to capture the relative smallness of the small parameters in this problem. We recall at this stage that $\alpha \ll 1$ but this is not a formal requirement to apply the multiple scale method. We also focus on small mistuning conditions, i.e. assume that the vortex shedding frequency of the fixed cylinder is close to the natural frequency of the structure. This is formalized by writing

$$\Omega = 1 + \xi\,\delta = 1 + \xi_0 \varepsilon\,\delta \quad \Leftrightarrow \quad \delta = \frac{\Omega - 1}{\xi} = \frac{f_{\text{shedding}} - f_0}{\xi\, f_0} \tag{8}$$

where $\delta \sim 1$ is a detuning parameter of order 1. This actually brings a total of 5 small numbers in this problem $\{I_u, \xi, \varepsilon, \alpha, \Omega - 1\}$; their smallness is fully exploited in order to derive simple analytical solutions of the stochastic governing equations.

Then the problem is reconsidered with the two timescales τ and $T = \varepsilon\tau$; derivatives are represented as partial derivatives and the solution is sought in the form of the following ansatz : $\mathcal{Y}(\tau;\varepsilon) = \mathcal{Y}_0\left[\tau, T(\tau);\varepsilon\right] + \varepsilon\mathcal{Y}_1\left[\tau, T(\tau);\varepsilon\right] + \cdots$, $\mathcal{Q}(\tau;\varepsilon) = \mathcal{Q}_0\left[\tau, T(\tau);\varepsilon\right] + \varepsilon\mathcal{Q}_1\left[\tau, T(\tau);\varepsilon\right] + \cdots$, where $\mathcal{Y}_i$ and $\mathcal{Q}_i$ $(i = 0, 1, \cdots)$ are of order 1. At leading order, the solution of the set of governing equations is

$$\mathcal{Y}_0 = R_y(T)\cos\left[\tau + \varphi(T)\right] \quad ; \quad \mathcal{Q}_0 = R_q(T)\cos\left[\tau + \varphi(T) + \psi(T)\right] \tag{9}$$

where the slowly varying amplitudes $R_y(T)$, $R_q(T)$ and the relative phase $\psi(T)$ satisfy the secularity equations (Denoël, 2020)

$$\begin{aligned} R_q' &= \mathcal{A}_0 R_y \sin\psi - \frac{1}{8}R_q^3 + \frac{1}{2}R_q \\ R_y' &= \mathcal{M}_0 R_q \sin\psi - \xi_0 R_y \\ \psi' &= \left(\mathcal{A}_0 \frac{R_y}{R_q} + \mathcal{M}_0 \frac{R_q}{R_y}\right)\cos\psi + \xi_0\delta + \mathcal{I}_0\mathcal{U} \end{aligned} \tag{10}$$

This set of governing equations shows that the presence of noise just affects the phase equation, at leading order. The closed-form solution of this set of equation remains challenging. The only possible approaches to its solution are numerical methods, based on Monte Carlo simulations, the associated Fokker-Planck-Kolmogorov equation or the moment equations and the closure method (but with a significant loss of accuracy).

In the unperturbed case ($\mathcal{I}_0 = 0$), the steady state solution is obtained by canceling the lefthand sides. This yields the limit cycle solution ($_{\text{LC}}$). From the second equation it is seen to satisfy

$$\left(\frac{R_y}{R_q}\right)_{\text{LC}} = \frac{\mathcal{M}_0}{\xi_0}\sin\psi_{\text{LC}}. \tag{11}$$

Substitution into the last equation indicates that the phase on the limit cycle $\cot\psi_{\text{LC}}$ satisfies

$$\cot^3\psi_{\text{LC}} + \delta\cot^2\psi_{\text{LC}} + (1 + \mathcal{D})\cot\psi_{\text{LC}} + \delta = 0 \tag{12}$$

where

$$\mathcal{D} := \frac{\mathcal{A}_0\mathcal{M}_0}{\xi_0^2} = \frac{\mathcal{A}_0\mathcal{M}_0}{\xi^2}\varepsilon^2 = \frac{2\mathcal{A}_0}{\varepsilon}\frac{1}{2\xi}\frac{\rho U_\infty^2 C_L^0}{8k_{\text{S}}}. \tag{13}$$

This shows that the phase on the limit cycle $\psi_{\mathsf{LC}} \equiv \psi_{\mathsf{LC}}(\delta, \mathcal{D})$ only depends on the mistuning δ and the dimensionless group $\mathcal{D}$. If the mistuning is small, the phase on the limit cycle is given by $\cot\psi_{\mathsf{LC}} \simeq -\delta/(1+\mathcal{D})$; this solution is valid if $|\delta| \ll 1+\mathcal{D}$. The dimensionless group $\mathcal{D}$ plays a significant role in the topology of the lock-in domain; it is possible to prove that the lock-in domain has a bell shape for $\mathcal{D} < 8$ and a mushroom shape for $\mathcal{D} > 8$ (Denoël, 2020). Once the phase on the limit cycle is known, the response envelopes on the limit cycle are obtained by $R_{q,\mathsf{LC}} = 2\sqrt{1+2\xi_0\mathcal{D}\sin^2\psi_{\mathsf{LC}}}$ and $R_{y_{\mathsf{LC}}} = \frac{\mathcal{M}_0}{\xi_0} R_{q,\mathsf{LC}} \sin\psi_{\mathsf{LC}}$.

3.3 The Slow phase model

Under a small perturbation, such as the small noisy forcing term, the trajectory of the system in the phase space only slightly deviates from the unperturbed limit cycle (because it is small and the cycle is stable). This deviation concerns the magnitude space variables but not the phase. In order to derive the slow phase dynamics of this problem, it is therefore possible to assume that the relation (11) which is a priori strictly valid on the limit cycle only also holds, at leading order, in the perturbed case. Its substitution in the third equation of the averaged model yields a simple first order equation for the phase

$$\psi' = \xi_0 \left(\mathcal{D}\sin\psi\cos\psi + \cot\psi + \delta\right) + \mathcal{I}_0\mathcal{U}. \tag{14}$$

Doing so, we have successively reduced the original 4-dimensional problem (6) to the 3-dimensional problem (10) and now to a 1-dimensional problem. Once the problem is solved for the phase, the response amplitudes are computed by

$$R_q = 2\sqrt{1+2\xi_0\mathcal{D}\sin^2\psi} \quad ; \quad R_y = 2\frac{\mathcal{M}_0}{\xi_0}\sin\psi\sqrt{1+2\xi_0\mathcal{D}\sin^2\psi} \tag{15}$$

where $R_q(T)$ and $R_y(T)$ are now time dependent. The *slow phase model* (14-15) not only provides a simple, although approximate, picture of the problem but is also a good candidate to explain with simple concepts and equations the influence of turbulence on a wake-oscillator model.

Using the change of variable $\Upsilon = \cot\psi$, the slow phase equation can be rewritten

$$\Upsilon' + \xi_0\delta + \xi_0(1+\mathcal{D})\Upsilon + \xi_0\delta\Upsilon^2 + \xi_0\Upsilon^3 = -\mathcal{I}_0\mathcal{U}\left(1+\Upsilon^2\right) \tag{16}$$

which is nothing but a first order stochastic differential equation with polynomial nonlinearity and parametric excitation. Despite the apparent simplicity of this stochastic differential equation, it appears that it has no simple explicit solution. In particular, Υ seems to be rather Gaussian for small $\mathcal{I}_0$ but gets heavily lemnikurtic as soon as $\mathcal{I}_0$ takes some moderate values. Any approach based on stochastic linearization or closure methods seems therefore inappropriate. However, a naive linearization method is applied in the following Section to derive a simple explicit solution.

3.4 Analytical model based on the slow phase model

The formal solution of (16) being deemed to be too cumbersome to be fully examined in the framework of this communication, the solution for small turbulence intensity is developed. In

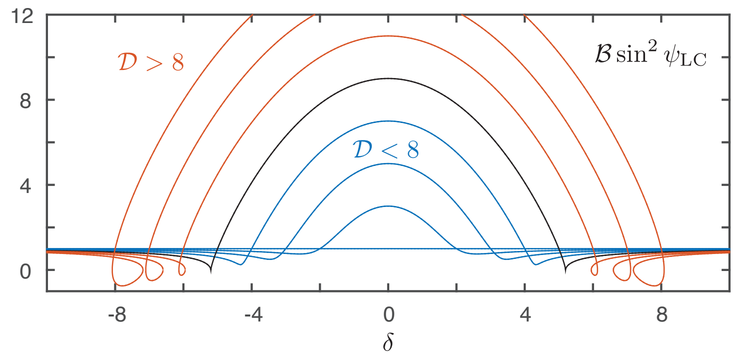

Figure 1: Influence of δ on the small intensity solution: plot of $\mathcal{B}\sin^2\psi_{\mathsf{LC}}$ as a function of δ. Shown for $\mathcal{D} = 2, 4, 6, 8, 10, 12, 14$.

the limit case where $\mathcal{I}_0 = I_u/\varepsilon$ is very small, the cotangent Υ of the phase remains close to its average value $\Upsilon_{\mathsf{LC}} = \cot\psi_{\mathsf{LC}}$. The deviation $\Delta\Upsilon = \Upsilon - \Upsilon_{\mathsf{LC}}$ from the phase of the limit cycle is governed by

$$\Delta\Upsilon' + \xi_0\mathcal{B}\,\Delta\Upsilon + \xi_0\left(\delta + 3\Upsilon_{\mathsf{LC}}\right)\Delta\Upsilon^2 + \xi_0\Delta\Upsilon^3 = -\mathcal{I}_0\mathcal{U}\left(1 + \left(\Upsilon_{\mathsf{LC}} + \Delta\Upsilon\right)^2\right) \tag{17}$$

where $\mathcal{B} = 1 + \mathcal{D} + 2\delta\Upsilon_{\mathsf{LC}} + 3\Upsilon_{\mathsf{LC}}^2$, which degenerates into

$$\Delta\Upsilon' + \xi_0\mathcal{B}\,\Delta\Upsilon = -\csc^2\psi_{\mathsf{LC}}\,\mathcal{I}_0\,\mathcal{U} \tag{18}$$

for small deviation $\Delta\Upsilon \ll 1$. This linear stochastic equation possesses a simple steady state solution. Its average value is $\mu_{\Delta\Upsilon} = 0$ (so $\mu_{\Upsilon} = \Upsilon_{\mathsf{LC}}$) and its power spectral density (PSD) is given by

$$S_{\Delta\Upsilon}\left(\omega_T\right) = \csc^4\psi_{\mathsf{LC}}\mathcal{I}_0^2\frac{S_{\mathcal{U}(T)}\left(\omega_T\right)}{\omega_T^2 + \xi_0^2\mathcal{B}^2} \tag{19}$$

where $\omega_T = \tilde{\omega}/\varepsilon$ is the circular frequency associated with the slow time T. The standard deviation of $\Delta\Upsilon$ is therefore given by

$$\sigma_{\Delta\Upsilon} = \frac{I_u}{\xi\mathcal{B}}\csc^2\psi_{\mathsf{LC}}\left(\int_{-\infty}^{+\infty}\frac{S_{\mathcal{U}}\left(\tilde{\omega};\alpha\right)}{1 + \left(\frac{\tilde{\omega}}{\xi\mathcal{B}}\right)^2}\mathrm{d}\tilde{\omega}\right)^{1/2}. \tag{20}$$

This equation is simple and rich at the same time; it is able to reproduce several features of the model. It is very useful once it is understood that small values of $\sigma_{\Delta\Upsilon}$ mean small deviations from the limit cycle and therefore small influence of the wind turbulence on the VIV response of the body. On the contrary, larger values of $\sigma_{\Delta\Upsilon}$ correspond to more frequent occurrences of phase slips and loss of synchronization. With this in mind, the model shows that

1. the mistuning δ influences the response through $\mathcal{B}$ (see definition above) and Υ_{LC}. For small values of $|\delta|$, $\mathcal{B}\sin^2\psi_{\mathsf{LC}}$ is larger than one ($\mathcal{B}\sin^2\psi_{\mathsf{LC}} = 1 + \mathcal{D}$ for $\delta = 0$); it also

decreases when $|\delta|$ goes away from 0, see Figure 1; as a result, $\sigma_{\Delta\Upsilon}$ is smaller in the center of the lock-in range and the turbulence makes it difficult to affect the VIV response in the center of the lock-in range;

2. $\sigma_{\Delta\Upsilon}$ is proportional to I_u; a larger turbulence intensity will therefore increase the phase shift and ultimately reduce VIV;

3. if $\alpha \gg \xi\mathcal{B}$, $\mathcal{V} \simeq 0$ and $\sigma_{\Delta\Upsilon}$ remains small; this means that the lock-in range and VIV response that are observed without turbulence remains unaffected by the turbulence in that case. In the limit case where the turbulence is modeled as a white noise ($\alpha \to +\infty$), there is no phase slip at all and the turbulence has no influence on the VIV response;

4. if $\alpha \ll \xi\mathcal{B}$, $\mathcal{V} \simeq 1$ and $\sigma_{\Delta\Upsilon}$ is governed by the first factors in (20); a reduction of VIV due to turbulence is therefore possible as per items discussed above.

As a conclusion, for turbulence to be able to tame VIV, it is necessary that the slow timescale of the turbulence be slower than the slow characteristic time of the problem and that the turbulence intensity be large enough. With dimensional variables, these conditions read

$$\alpha \lesssim \xi\mathcal{B} \quad \Leftrightarrow \quad a \lesssim \xi\omega_0 \left(1 + \mathcal{D} + 2\delta\Upsilon_{\mathrm{LC}} + 3\Upsilon_{\mathrm{LC}}^2\right) \tag{21}$$

$$\frac{I_u}{\xi\mathcal{B}} \csc^2 \psi_{\mathrm{LC}} \sim 1 \quad \Leftrightarrow \quad I_u \lesssim \xi\,\mathcal{B} \sin^2 \psi_{\mathrm{LC}} \tag{22}$$

where a is the dimensional characteristic frequency of turbulence (center of gravity in the PSD of $\mathcal{U}(\tau)$). The second condition being dependent on δ, the influence of turbulence on the VIV response differently affects the center of lock-in range (less affected) and the borders of the lock-in range.

4 Illustrations

The derivation of the above relations is illustrated with a turbulence assumed to be a random process with decreasing exponential autocorrelation. The power spectral density of this stochastic process, in dimensionless variables, reads

$$S_{\mathcal{U}}\left(\tilde{\omega}; \alpha\right) = \frac{\alpha}{\pi} \frac{1}{\tilde{\omega}^2 + \alpha^2} \tag{23}$$

where α is the parameter quantifying the relative magnitude between the timescale (period) of the oscillator and the timescale of turbulence. In typical applications, this ratio is very small, in the range $[10^{-4}; 5 \cdot 10^{-2}]$. In the following illustration, the turbulence intensity I_u is considered as a parameter; it is varied in the range [0,20%] in order to illustrate the smooth transition from perfect locked-in conditions to unlocked conditions, as a result of the perturbing stochastic action of turbulence. The other numerical values chosen in the illustration are summarized in Table 1.

A first reference solution is obtained by simulating the original problem (6). Samples of the wind turbulence are generated, then the fast dynamics of the coupled system are resolved and integrated. Very long time series covering $25,000$ cycles are simulated in order to provide

ε	ξ_s	ξ_a	α	$\mathcal{M}_0$	$\mathcal{A}_0$
0.05	0.015	0.015	0.002	0.9	1
	I_u	ξ_0	$\mathcal{D}$	$\xi(1+\mathcal{D})$	
	variable	0.6	2.5	$\Delta\Omega = \pm 0.105$	

Table 1: Typical range of variation of the parameters of the problem and considered numerical values in the illustrations.

accurate statistics. In this fast unresolved dynamical approach, a time step of $\Delta\tau$ =0.01 is chosen in order to accurately represent the solution. This serves as a reference solution for the other two models. The resulting solution is represented by black lines in Figure 2. This Figure shows the histogram of the structural response $y/D = \varepsilon\mathcal{Y}$ for two values of the mistuning δ and three values of the turbulence intensity. For small turbulence intensity (I_u =5%, on the left), the maximum response is close to $y_{\max}/D = 0.3$ which corresponds to the limit cycle amplitude in the absence of turbulence. As turbulence increases, phase slips occur and the structural response is more often far from ideal locked-in conditions, which explains why the histogram of the response smoothly relocates towards small values.

The second solution (red lines) is obtained by simulating the averaged model (10) instead of the original one. As is well known in perturbation theories and also recently discussed in wind engineering applications (Mannini, 2020), the averaging procedure does a pretty good job as soon as $\varepsilon \ll 1$. In this case, ε is chosen equal to 0.05; it is therefore expected that these results match those of the original problem. An important difference though concerns the fact that these results do not require now to resolve the fast dynamics since only the envelope is computed. This is an major advantage of the averaged model over the original one, especially as soon as statistics of a stationary response (in the sense of stochastic processes) have to be determined.

The third solution (blue lines) corresponds to the slow phase model proposed in (Denoël, 2020). These results have been obtained by numerical simulation of the slow phase model (14), then substitution into (15) in order to get the time series of R_y which are ultimately treated by means of a statistical analysis to yield the histograms of y/D. The results do compare again reasonably well with the reference solution, despite the additional hypothesis that the stochastic response evolves in a neighborhood of the limit cycle has been formulated. The slow phase model successfully captures the transition from locked-in ($I_u = 5\%$) to unlocked conditions ($I_u = 20\%$). The little conservatism associated with a small probability in the neighborhood of $y/D = 0.3$ is noticeable but also negligible. The transition is better captured in the bulk of the lock-in range, when $\delta = 0$.

At last but not least, the proposed analytical formulation, based on a transition layer approximation derived from (20), see (Denoël, 2020), is used to determine the average and standard deviation of $\Delta\Upsilon$, in closed form. Once this is done, the statistics of $\Delta\Upsilon$ is fed into the memoryless model (15) in order to obtain the statistics of R_y. In order to ease comparison, they are also represented as histograms in Figure 2. Although the transition from locked-in to unlocked is still quite reasonably captured, the discrepancy with the exact solution is increased. This is a result of the assumption of Gaussianity for $\Delta\Upsilon$.

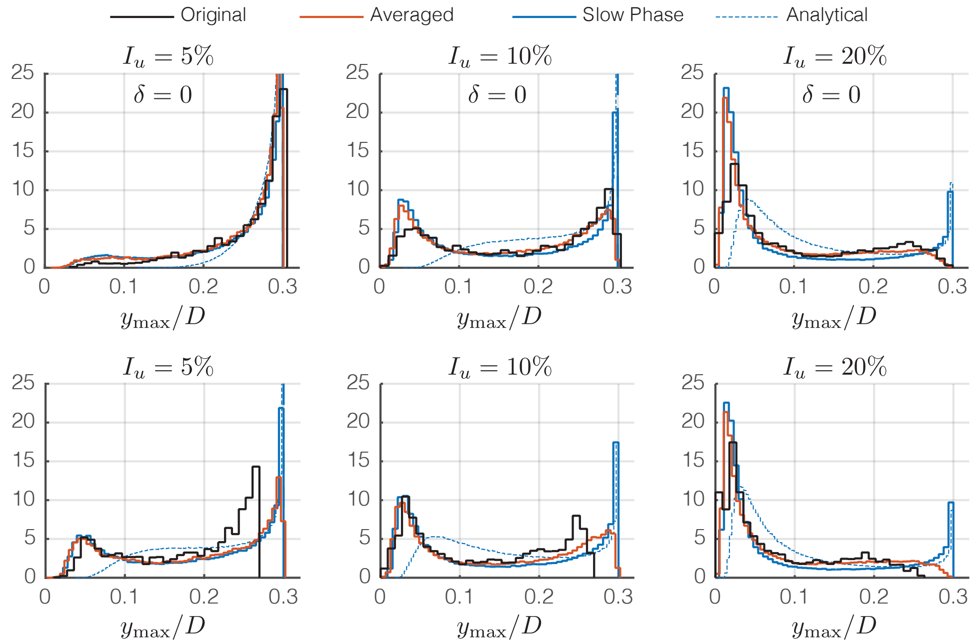

Figure 2: Comparison of the probability density function of the envelope of the structural response R_y, obtained with the 4 models described in this paper: (1) the original model (6), the averaged model (10), the slow phase model (14-15) and the analytical formulation corresponding to the small intensity asymptotic solution of the slow phase model (20), combined with (15). Top line $\delta = 0$, bottom line $\delta = 2$. Other numerical values given in Table 1.

5 Conclusions

The paper has summarized and illustrated the development of a slow phase model of vortex induced vibrations in turbulence conditions. This model assumes a slow envelope of the stochastic response and considers that the dynamics of the forced system evolves in the neighborhood of the limit cycle (which is in fact similar to exploiting the slowness of the turbulence $\alpha \ll 1$). The slow phase model is governed by a first order nonlinear stochastic equation. Its solution is simple in some limiting cases, which have been illustrated in this paper. These solutions can be used to understand the way this phenomenological model attempts to model the influence of turbulence on the mitigation of VIV: turbulence drives the system away from the limit cycle, not in terms of magnitude, but well in terms of phase. The turbulence therefore contributes to drive the phase away from optimal locked-in conditions. Phase slips and accumulation thereof are then responsible for a decrease of energy pumped into the structural degree-of-freedom, causing therefore the reduction of response due to turbulence. With this simple model, it has been shown that the timescale of the turbulence needs to be slow enough, see (21), for the turbulence to have an influence. A second necessary condition is related to the magnitude of the turbulence intensity which needs to be large enough, see (22).

References

V. Denoël, "Stochastic slow phase model of vortex-induced vibrations", Submitted to Journal of Fluids and Structures, Feb. 2020.

V. Denoël (2015). Multiple timescale spectral analysis. Probabilistic Engineering Mechanics, 39, 69-86.

V. Denoël, & Carassale, L. (2015). Response of an oscillator to a random quadratic velocity-feedback loading. Journal of Wind Engineering and Industrial Aerodynamics, 147, 330-344.

M. L. Facchinetti, E. De Langre, Emmanuel, F. Biolley, Coupling of structure and wake oscillators in vortex-induced vibrations, Journal of Fluids and structures 19, 2 (2004), pp. 123--140.

I. Goswami, R. H Scanlan, and N. P Jones. Vortex-induced vibration of circular cylinders. i: experimental data. Journal of Engineering Mechanics, 119(11):2270–2287, 1993.

Hinch, E. J. Perturbation methods. 1991.

C. Mannini, T. Massai, A. M. Marra (2018). Modeling the interference of vortex-induced vibration and galloping for a slender rectangular prism. Journal of Sound and Vibration, 419, 493-509.

C. Mannini, (2020). Asymptotic Analysis of a Dynamical System for Vortex-Induced Vibration and Galloping. In Nonlinear Dynamics of Structures, Systems and Devices (pp. 389-397). Springer, Cham.

D. T. Nguyen, D. M. Hargreaves, J. S. Owen (2018). Vortex-induced vibration of a 5: 1 rectangular cylinder: a comparison of wind tunnel sectional model tests and computational simulations. Journal of Wind Engineering and Industrial Aerodynamics, 175, 1-16.

M. P. Païdoussis, S. J. Price, De Langre, E. (2010). Fluid-structure interactions: cross-flow-induced instabilities. Cambridge University Press.

A. Pikovsky, M. Rosenblum, J. Kurths (2003). Synchronization: a universal concept in nonlinear sciences (Vol. 12). Cambridge university press.

Y. Tamura (1981). Wake-oscillator model of vortex-induced oscillation of circular cylinder. Journal of Wind Engineering, 1981(10), 13-24.

B.J. Vickery and A.W. Clark, "Lift or across-wind response of tapered stacks", Journal of Structural Division, ASCE, Vol. 98, pp. 1-20, 1972.

B.J. Vickery and R.I. Basu, "Across-wind vibrations of structures of circular cross-section. Part 1. Development of a mathematical model for two-dimensional conditions", Journal of Wind Engineering and Industrial Aerodynamics, Vol. 12, pp. 49-73, 1983.